

****TITLE****

*ASP Conference Series, Vol. **VOLUME**, **PUBLICATION YEAR***

****EDITORS****

Properties of a Chemically Enriched Ly α Absorption System at $z = 0.167$ and Implications for the Total Baryons in Extended Gaseous Envelopes Around Galaxies

Hsiao-Wen Chen and Jason X. Prochaska

Carnegie Observatories, 813 Santa Barbara St., Pasadena, CA 91101

Kenneth M. Lanzetta

Physics and Astronomy Department, SUNY at Stony Brook, Stony Brook, NY 11794-3800

Abstract.

We present a detailed analysis of the chemical abundances, ionization state, and origin of a partial Lyman limit system ($N(\text{H I}) \approx 10^{16} \text{ cm}^{-2}$) at low redshift ($z = 0.167$ towards PKS0405–1219). We also present the first estimate of the total baryons in extended gaseous envelopes around galaxies based on a simple photoionization model for the Ly α absorbers. We find that extended gaseous envelopes can explain between 5–20% of the total baryons predicted by the big bang nucleosynthesis model.

1. Background

Various studies have shown that the “forest” of Ly α absorption lines observed in the spectra of background QSOs are a sensitive probe of the physical conditions of intervening gas (e.g. Rauch 1998). Comparisons of galaxies and QSO absorption systems along common lines of sight, therefore, allow us not only to determine the origin of QSO absorption systems but also to study properties of tenuous gas around galaxies at large distances. Over the past several years, studies of faint galaxies in QSO fields have demonstrated that galaxies of a wide range of luminosity and morphological type possess extended gaseous envelopes of radius $\sim 180 h^{-1} \text{ kpc}$ and that known galaxies of known gas cross section can explain most and perhaps all of Ly α absorption systems of $N(\text{H I}) \gtrsim 10^{14} \text{ cm}^{-2}$ (Lanzetta et al. 1995; Chen et al. 1998, 2001). A more detailed review of the relationship between Ly α absorption systems and galaxies is presented by Lanzetta in these proceedings. Here we summarize the main reasons that support this conclusion as following:

1. The galaxy-absorber cross-correlation function exhibits a strong amplitude on velocity scales of $\lesssim 250 \text{ km s}^{-1}$ and impact parameter scales of $\lesssim 200 h^{-1} \text{ kpc}$, and becomes diminishingly small at impact parameters beyond $200 h^{-1} \text{ kpc}$ on all velocity scales (Lanzetta, Webb, & Barcons 1997). This indicates that Ly α absorption systems strongly cluster around galaxies on dynamical scales of individual galaxies, rather than on scales of large filamentary structures.

2. There exists a strong anti-correlation between Ly α absorption equivalent width and galaxy impact parameter. Namely, galaxies at larger impact parameters are found to be associated with weaker Ly α absorption systems. Including the intrinsic luminosities of individual galaxies as an additional scaling factor further improves the anti-correlation between Ly α absorption equivalent width and galaxy impact parameter, indicating that the extent of tenuous gas around galaxies scales with individual galaxy luminosity/mass (Chen et al. 1998, 2001).

3. Almost all galaxies that are at $\delta v \gtrsim 3000 \text{ km s}^{-1}$ away from the background QSOs and at $\rho \lesssim 200 h^{-1} \text{ kpc}$ produce associated Ly α absorption lines, indicating that the covering factor of tenuous gas around galaxies is approximately unity (Lanzetta et al. 1995; Chen et al. 1998, 2001). On the contrary, almost all galaxies that are in the vicinities of the background QSOs ($\delta v \lesssim 3000 \text{ km s}^{-1}$ and $\rho \lesssim 200 h^{-1} \text{ kpc}$) do not produce associated Ly α absorption lines to within sensitive upper limits, consistent with the picture that tenuous gas around these galaxies are highly ionized due to an enhanced ionizing radiation intensity from the background QSOs (Pascarelle et al. 2001).

By combining results of previous studies of extended Mg II, C IV, and Ly α gas around galaxies (derived based on analyses of QSO absorption systems), we can establish a schematic picture of the structure of extended gas around galaxies: A typical L_* galaxy is surrounded by high column density gas of radius a few tens kpc (e.g. van Gorkom 1993), which, because of its high density, remains mostly neutral. The gas becomes more ionized as the gas density decreases with increasing galactic radius. Low-ionization species, such as singly ionized magnesium Mg II, become the dominant observational signature out to $\approx 50 h^{-1} \text{ kpc}$ (e.g. Bergeron & Boissé 1991). As the gas density continues to decline at larger galactic radii, the gas becomes still more highly ionized. High-ionization species, such as triply ionized carbon C IV, become the dominant observational signature out to $\approx 100 h^{-1} \text{ kpc}$, at neutral hydrogen column densities $N(\text{H I}) \approx 10^{16} \text{ cm}^{-2}$ (Chen, Lanzetta, & Webb 2001). The tenuous gas continues to extend to at least $\approx 180 h^{-1} \text{ kpc}$, at neutral hydrogen column densities at least as low as $N(\text{H I}) \approx 3 \times 10^{14} \text{ cm}^{-2}$ (Chen et al. 1998, 2001). This picture applies to galaxies of a wide range of luminosity and morphological type.

There is, however, a lack of understanding of the physical properties of extended gas at large galactic distances, such as number density, ionization state, and metallicity, because of limited information regarding kinematics and metallicity of the gas. The primary difficulty arises in acquiring a high-quality QSO spectrum of wide UV spectral coverage. Here we present an analysis of the chemical abundances, ionization state, and origin of a partial Lyman limit system (LLS; $N(\text{H I}) \approx 10^{16} \text{ cm}^{-2}$) at low redshift ($z = 0.167$ towards PKS0405–1219). Combining the results of our analysis for the $z = 0.167$ system with those for high-redshift Ly α absorption systems obtained in the literature, we also present the first estimate of the total baryons in extended gaseous envelopes around galaxies based on a simple photoionization model.

2. The Partial Lyman Limit System at $z = 0.167$

The absorption system at $z = 0.167$ toward PKS0405–1219 ($z_{em} = 0.5726$) was first identified in an HST/FOS spectrum with a rest-frame Ly α absorption

equivalent width of 0.65 Å and a rest-frame CIV absorption equivalent width of 0.44 Å. Subsequent echelle spectroscopy with HST/STIS further revealed absorption features produced by H⁰ (Lyβ), C⁺, N⁺, O⁰, Si⁺, Si⁺⁺, Si⁺³, possibly Fe⁺ and Fe⁺⁺; and most interestingly absorption doublets produced by N⁺⁴ and O⁺⁵ at the redshift of the absorption system. We estimated the physical properties of the absorption system based on both photoionization and collisional ionization models, using the relative abundance ratios between different transitions. Detailed analysis has been presented in Chen & Prochaska (2000). We summarize the results here.

First, all the ions except N⁺⁴ and O⁺⁵ showed consistent profile signatures that trace the partial LLS, while the NV and O VI doublets appeared to be broad with velocity centroids blue-shifted by $\approx 30 \text{ km s}^{-1}$ from the other ions. The differences in kinematic signatures strongly indicate that the NV and O VI doublets and the partial LLS traced by the other ions do not arise in the same regions (see Figure 1 in Chen & Prochaska 2000).

Second, metals that are associated with the partial LLS showed a wide range of ionization state. We present the column density measurements in Table 1, which lists the ions, the corresponding rest-frame absorption wavelength λ_0 , and the estimated ionic column densities $\log N$ together with the associated errors in the first three columns. The comparable abundances between various Si ions indicate that the partial LLS is photoionized.

Table 1. Measurements of Column Densities, Doppler Parameters, and Abundances

Species	λ_0	$\log N \text{ (cm}^{-2}\text{)}^a$	$b \text{ (km s}^{-1}\text{)}$	$[\text{X}/\text{H}]^b$
H I ...	1025.72	> 15.7	34.7 ± 2.5	...
	1215.67	> 15.7
C II ...	1036.79	> 14.10
	1334.53	14.27 ± 0.09	...	-0.33
N II ..	1083.99	> 14.25	11.6 ± 1.0	0.27
N V ..	1238.82	13.84 ± 0.07	50.2 ± 7.0	...
	1242.80	13.91 ± 0.06
O I ...	1302.17	13.68 ± 0.14	...	0.25
O VI ..	1031.93	14.67 ± 0.16	72.6 ± 4.9	...
	1037.62	14.76 ± 0.07
Si II ..	1190.42	13.22 ± 0.07	9.9 ± 0.9	...
	1193.29	13.29 ± 0.05
	1260.42	> 13.16
	1304.37	13.40 ± 0.12	...	-0.37
Si III .	1206.50	> 13.33	...	> -0.76
Si IV .	1393.76	13.18 ± 0.05
	1402.77	13.49 ± 0.07	...	-0.45

^aLower limits indicate that the lines are saturated.

^b $[\text{X}/\text{H}]$ is defined as $\log [N(\text{X})/N(\text{H})] - \log [\text{X}/\text{H}]_{\odot}$.

Third, comparisons of the relative abundances of the Si ions and predictions based on a series of photoionization models calculated using the CLOUDY software package (Ferland 1995) showed that the ionization parameter, which is the ratio of incident ionizing photons at 912 Å to the total hydrogen number density,

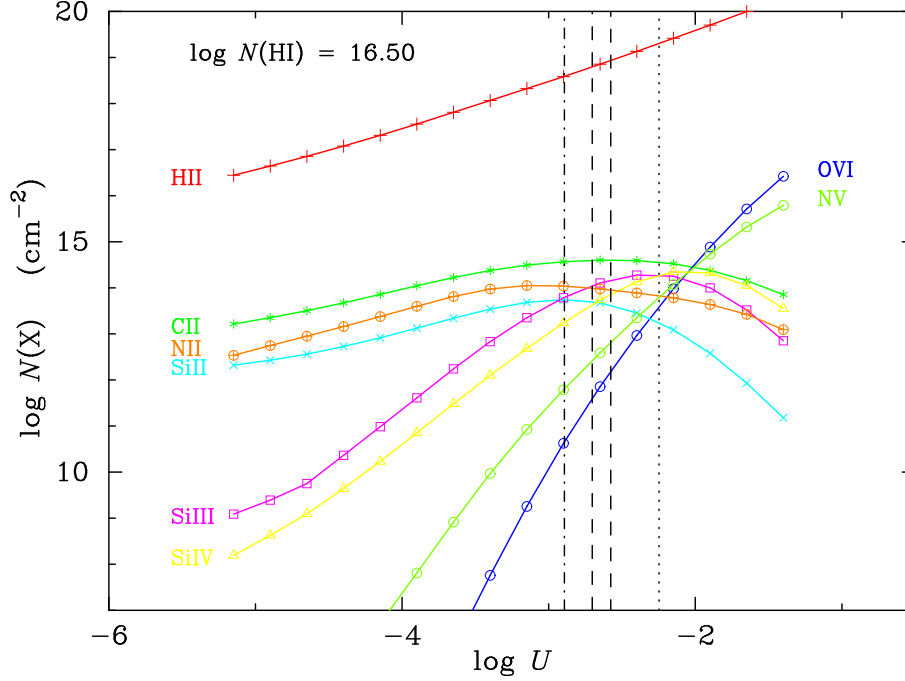


Figure 1. Predicted relative abundances of various ions X for a plane-parallel slab of absorbing gas of solar metallicity based on a photoionization analysis using CLOUDY. The dashed lines indicate the plausible range of the ionization parameter U determined using the observed abundance ratios between Si^+ and Si^{+3} for the system at $z = 0.167$; the dotted and dot-dashed lines indicated the lower and upper limits of U determined based on the ratios of $\text{Si}^{++}/\text{Si}^+$ and $\text{Si}^+/\text{Si}^{++}$.

$U \equiv \phi_{912}/cn_{\text{H}}$, was constrained to be $\log U = -2.64 \pm 0.07$. In addition, the observed abundances of the N^{+4} and O^{+5} ions cannot be explained by the same photoionization models (Figure 1). For an extreme upper limit $\log U = -2.2$, both O VI and NV were predicted to be at least 0.4 dex less abundant than Si IV, while our measurements showed that O VI and NV are at least 0.4 dex more abundant than all the Si ions. This result, together with their kinematic signature, indicates that these ions arise in a different region and suggests that they may be collisionally ionized.

Fourth, the temperature of the partial LLS was found to be $T \approx 7.4 \times 10^4$ K with a 1σ lower limit being $T \approx 2.7 \times 10^4$ K and 1σ upper limit being $T \approx 1.5 \times 10^5$ K, using the Doppler parameters b estimated from a Voigt profile analysis (column 4 of Table 1) for the unsaturated lines produced by Si^+ and N^+ . Because the cooling function is the most effective at $T \approx 10^5$ K (see e.g. Spitzer 1978), the temperature of the partial LLS is more likely to be a few times 10^4 K.

Fifth, assuming that the more highly ionized component traced by the O^{+5} and N^{+4} ions is collisionally ionized, we estimated the temperature to be $T = (2.6 \pm 0.1) \times 10^5$ K by comparing the observed O VI and NV column density ratio with predictions based on a series of collisional ionization models presented in

Shapiro & Moore (1976). In order for the hot gas to remain at this temperature, we further estimated the mass of the galaxy or galaxy group that supports the extended hot gas to be $\approx 1.5 \times 10^{12} M_{\odot}$, assuming a simple isothermal profile of a half-mass radius $r_h \approx 0.35$ Mpc. By requiring a cooling time longer than the dynamical time, we estimated the number density of the absorbing gas should be $\lesssim 3 \times 10^{-5} \text{ cm}^{-3}$.

Finally, we estimated the elemental abundances of the partial LLS using the ionization fraction correction calculated from the CLOUDY model for an ionization parameter $\log U = -2.64$. In addition, we also estimated the chemical abundance using the [O I/ H I] column density ratio, which is a direct estimate of the oxygen elemental abundance in regions where the resonant charge-exchange reaction between oxygen and hydrogen becomes dominant. The results are shown in the last column of Table 1 for an H I column density $\log N(\text{H I}) = 16.5$. It shows that the partial LLS would have 1/10 solar abundance determined for carbon and silicon, 1/5 solar abundance for nitrogen, and at least 1/2 solar for oxygen. Increasing (decreasing) $N(\text{H I})$ by 0.5 dex decreases (increases) the abundance measurements by 0.5 dex.

To summarize, the Ly α absorption system at $z = 0.167$ is a chemically enriched partial LLS that exhibits a wide range of ionization state and is likely to be embedded in a more wide-spread, collisionally ionized hot gas that gives rise to the absorption features of O $^{+5}$ and N $^{+4}$. A summary of the physical parameters of the warm and hot gas that are associated with this system is presented in Table 2 of Chen & Prochaska (2000). Ground-based galaxy surveys (Spinrad et al. 1993; Ellingson & Yee 1994) of the field surrounding PKS0405–1219 have found an elliptical galaxy at $z = 0.1667$ and impact parameter $\rho = 74.9 h^{-1} \text{ kpc}$ with a rest-frame K -band luminosity $L_K = 1.20 L_{K*}$ and (2) a spiral galaxy at $z = 0.1670$ and at $\rho = 62.8 h^{-1} \text{ kpc}$ with $L_K = 0.02 L_{K*}$. By carefully examining deep optical and near-infrared images, we find that if there are unidentified dwarf galaxies at the absorber redshift and closer to the QSO line of sight, then they cannot be brighter than $0.02 L_{K*}$. By applying the luminosity scaled anti-correlation between Ly α absorption strength and galaxy impact parameter presented in Chen et al. (2001), we find that the elliptical galaxy alone can easily explain the amount of absorption. While it is not uncommon to find tenuous gas at large galactic distance ($\rho \sim 100 h^{-1} \text{ kpc}$) around nearby elliptical galaxies (e.g. Fabbiano, Kim, & Trinchieri 1992) or in groups of galaxies (e.g. Mulchaey et al. 1996), it is surprising to find metal-enriched, high-column density gas at this large distance. The spectral characteristics of the elliptical galaxy exhibit signs of recent star formation (Spinrad et al. 1993), therefore the physical process that initiated the recent star formation might be responsible for transporting metals to large galactic distance.

3. Total Baryons in Extended Gaseous Envelopes Around Galaxies

Big bang nucleosynthesis (BBN) makes specific predictions for the light element abundances (D, ^3He , ^4He , and ^7Li) as a function of the nucleon to proton ratio η (e.g. Schramm & Turner 1998). Abundance measurements of these elements determine η and therefore reveal the mean baryon density Ω_b in the universe when combined with measurements of the cosmic background radiation. Measure-

ments of the deuterium abundance along three sightlines toward high-redshift QSOs have yielded a precise estimate of the baryon density of $\Omega_b h^2 = 0.02$ (e.g. Burles, Nollett, & Turner 2001). Combined data from various cosmic microwave background experiments have also shown exciting agreement in the estimate of Ω_b (e.g. Wang, Tegmark, & Zaldarriaga 2001). The consistent results in Ω_b greatly increase the confidence in our current understanding of the formation of the universe. While all the baryons may be accountable by the Ly α forest at high redshifts (Rauch et al. 1997), it has, however, been shown that the sum of all the baryons seen in different environment only makes up 1/3 of the total baryons predicted by BBN (Fukugita, Hogan, & Peebles 1998). Finding the missing baryons is therefore crucial for establishing a complete picture of the formation and evolution of the universe.

Fukugita et al. (1998) attributed the “missing baryons” to the hot gas around galaxy groups with temperatures $\approx 10^5$ K, a temperature range that is out of reach by existing X-ray facilities but may be probed using the O VI absorption systems observed in the spectra of background QSOs (Mulchaey et al. 1996). Results of hydrodynamic simulations also suggested that 30%–40% of the total baryons are in ionized gas of temperatures between 10^5 and 10^7 K at low redshifts (Cen & Ostriker 1999; Davé et al. 2001). Recent analysis of intervening O VI absorption systems indeed showed evidence that supports a significant baryon reservoir in the hot gas probed by the O VI absorbers (Tripp, Savage, & Jenkins 2000). There is, however, a large uncertainty due to poor statistics in the line densities of the O VI absorption systems and unknown gas properties such as metallicity and ionization fraction of the gas. In addition, some fraction of the Ly α forest have associated O VI absorption lines, a simple addition of the total baryon contributions from the two species will result in a double-counting error (see the contribution by Tripp in these proceedings).

Because extended gaseous envelopes are a common and generic feature of galaxies of a wide range of luminosity and morphological type (Chen et al. 1998, 2000), some fraction of the total baryons must reside in the gaseous envelopes of individual galaxies that have not been counted in previous measurements. Here we present the first estimate of the total baryons in tenuous gas around galaxies on the basis of known galaxies that are represented by a galaxy luminosity function and of known gaseous extent of these galaxies. Our analysis takes advantage of better known galaxy statistics and is based on hydrogen directly. It requires an accurate estimate of the ionization fraction of the tenuous gas, but it does not require knowledge of the metallicity of the gas.

To determine the ionization fraction of an absorber requires high-resolution, high-sensitivity QSO spectroscopy to identify associated metal lines in the rest-frame UV spectral range. A handful of Ly α absorption systems have so far been studied extensively for the ionization state of the absorbing gas (Bergeron et al. 1994; Lopez et al. 1999; Prochaska 1999; Prochaska & Burles 1999; Rauch et al. 1999), in addition to the partial LLS at $z = 0.167$. All of these absorption systems are best explained by a simple photoionization model, in which the ionization fraction of the gas clouds only depends on the ionization parameter U . Adopting a best estimate of the ionizing flux intensity J_{912} for a gas cloud of known geometry, we can therefore infer the ionization fraction for a Ly α absorber of a given neutral hydrogen column density.

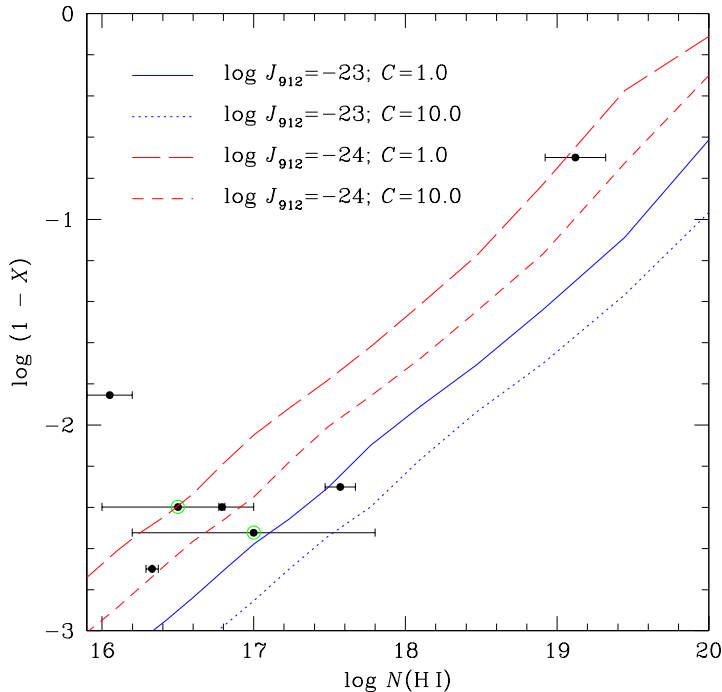


Figure 2. Comparisons of estimated ionization fraction for seven Ly α absorption systems and predictions based on a series of photoionization models. Points with circles indicate the two absorbers at $z < 1$. Curves indicate predicted ionization fraction as a function of neutral hydrogen column density $N(\text{H I})$ for a range of ionizing flux intensity J_{912} at 912 Å and a range of neutral hydrogen clumping factor C .

Figure 2 shows the predicted ionization fraction $X \equiv N(\text{H}^+)/N(\text{H})$ as a function of neutral hydrogen column density $N(\text{H I})$ (curves) obtained using CLOUDY for a range of J_{912} . Estimates of a handful Ly α absorption systems obtained from the literature are shown in closed points with the two $z < 1$ systems highlighted in circles (the $z = 0.167$ system described in § 2 and the $z = 0.79$ system studied by Bergeron et al. 1994). We have also included a clumping factor $C = \sqrt{\langle n_{\text{HI}}^2 \rangle} / \langle n_{\text{HI}} \rangle^2$, where n_{HI} is neutral hydrogen number density, in the models to account for the clumpiness of the gas. Comparisons of various models show that a higher J_{912} would imply a lower C and vice versa for a system with known X and $N(\text{H I})$. Given that the background ionizing radiation intensity evolves rapidly with redshift (e.g. Haardt & Madau 1996), we determine a best-fit range in J_{912} and C based only on the two $z < 1$ points. We find that it is *unlikely* to have $J_{912} \gtrsim 10^{-23}$ ergs sec $^{-1}$ cm $^{-2}$ Hz $^{-1}$ Sr $^{-1}$ and $C \gtrsim 10$ for these low-redshift absorbers. If we adopt the best estimated J_{912} obtained from the QSO proximity effect measurements (Pascarelle et al. 2001; Scott & Bechtold in these proceedings), $0.5\text{--}1 \times 10^{-23}$ ergs sec $^{-1}$ cm $^{-2}$ Hz $^{-1}$ Sr $^{-1}$, then we find a clumping factor of order unity.

To estimate the total baryons in extended gaseous envelopes of galaxies, we first determine the total hydrogen number density profiles of individual galaxies.

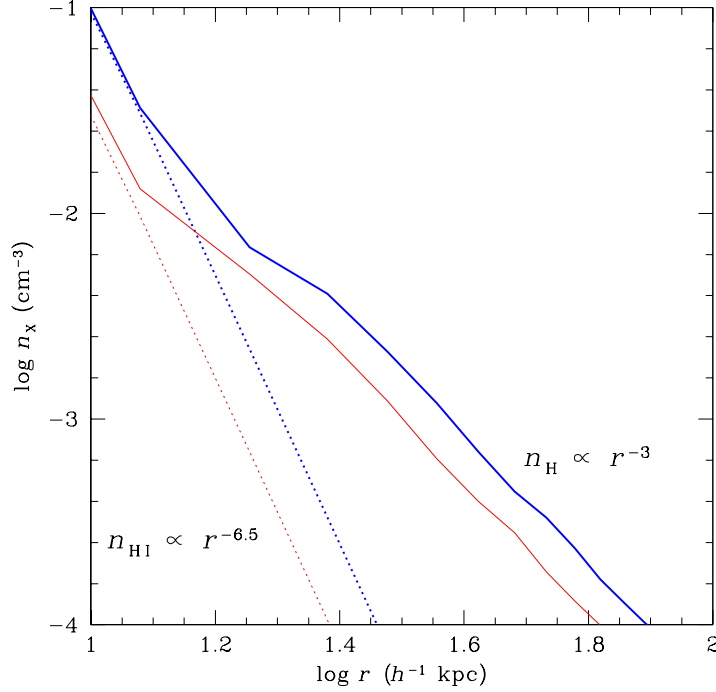


Figure 3. Hydrogen density profiles of a typical L_* galaxy, assuming $J_{912} = 10^{-23}$ ergs sec $^{-1}$ cm $^{-2}$ Hz $^{-1}$ Sr $^{-1}$. Thick curves are for $C = 1$; thin curves are for $C = 10$. Solid curves indicate the estimated total hydrogen profile; dotted curves indicate the neutral hydrogen profiles. It shows that extended gas is mostly neutral at $r \lesssim 15 h^{-1}$ kpc and therefore neutral hydrogen traces the total hydrogen gas profile. At $r \gtrsim 15 h^{-1}$ kpc, extended gas becomes highly ionized. While the neutral hydrogen gas profile appears to be as steep as $n_{\text{HI}} \propto r^{-6.5}$, the total gas density profile is well represented by $n_{\text{H}} \propto r^{-3}$.

Adopting the neutral hydrogen column density profile in Chen et al. (2001),

$$N_{\text{HI}}(\rho, L_B) = 3.63 \times 10^{21} \left(\frac{\rho}{10 \text{ kpc}} \right)^{-5.56 \pm 0.42} \left(\frac{L_B}{L_{B*}} \right)^{2.56 \pm 0.43} \text{ cm}^{-2}, \quad (1)$$

we derive the underlying neutral hydrogen number density profile, according to

$$n_{\text{HI}}(r, L_B) = -\frac{1}{\pi C} \int_r^\infty \frac{dN_{\text{HI}}(\rho, L_B)}{d\rho} \frac{d\rho}{\sqrt{\rho^2 - r^2}}. \quad (2)$$

To derive a total hydrogen number density profile, we apply proper ionization corrections determined from the CLOUDY photoionization calculations for gas of a given n_{HI} . The results are shown in Figure 3 for extended gas around a typical L_* galaxy. It shows that extended gaseous profiles may be well described by a power-law r^α with $\alpha \approx -3$, which is steeper than the one expected from an isothermal equilibrium model but agrees well with expectation from a dissipational formation scenario (Silk & Norman 1981).

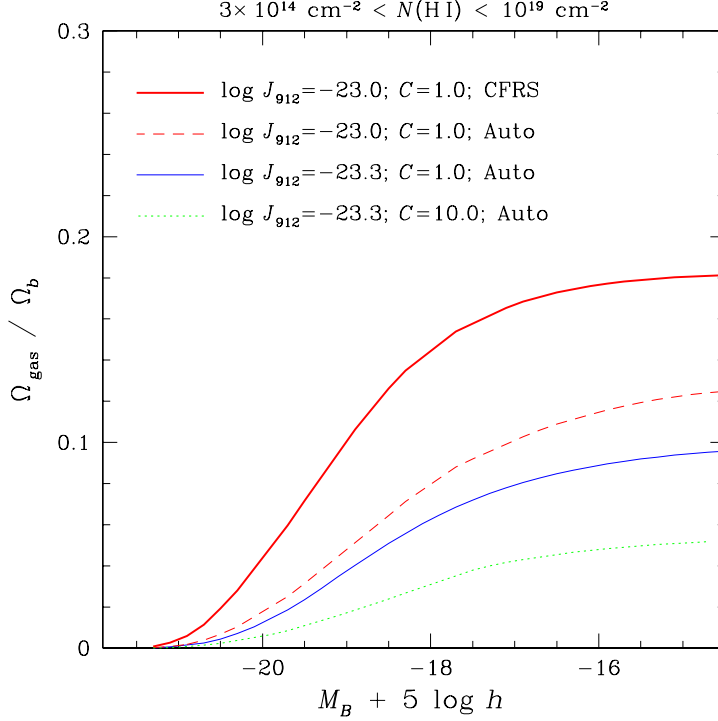


Figure 4. Cumulative contribution of baryons in extended gaseous envelopes of galaxies of different luminosity. The calculations are for regions that correspond to $3 \times 10^{14} \text{ cm}^{-2} \lesssim N(\text{H I}) \lesssim 10^{19} \text{ cm}^{-2}$.

Next, we calculate the cumulative contribution of baryons in extended gaseous envelopes from galaxies of different luminosity according to

$$\Omega_b \equiv \frac{\rho_b}{\rho_c} = \frac{4\pi\mu m_{\text{H}}}{\rho_c} \int \phi\left(\frac{L_B}{L_{B*}}\right) d\left(\frac{L_B}{L_{B*}}\right) \int_{r_1}^{r_2} r^2 n_{\text{H}}(r, L_B) dr, \quad (3)$$

where μ is the mean atomic weight, m_{H} is the proton mass, ρ_c is the present-day critical mass density, and ϕ is the galaxy luminosity function. The limits of the integral (r_1, r_2) correspond to the column density interval of interest here with the lower limit $N(\text{H I}) = 3 \times 10^{14} \text{ cm}^{-2}$ set by the sensitivity of the galaxy survey from which equation (1) was determined.

Given the uncertainties in the galaxy luminosity function measurements, we calculate equation (3) using results from the CFRS (Lilly et al. 1995) and Autofib (Ellis et al. 1996) surveys. The results are shown in Figure 4. It shows that extended gaseous envelopes of luminous galaxies ($M_B \lesssim M_{B*}$) contribute most of the baryons, as indicated by the flattening of the curves toward fainter magnitudes beyond L_* . The luminosity function of Lilly et al. has a higher normalization in galaxy number density and a shallower faint-end slope than that of Ellis et al., and hence gives a higher value of Ω_{gas} . For a range of J_{912} and C , we find that $\approx 5\text{--}20\%$ of the total baryons predicted by BBN are in extended gaseous envelopes of galaxies.

References

- Bergeron, J. & Boissé, P. 1991, *A&A*, 243, 344
- Bergeron, J., Petitjean, P. et al. 1994, *ApJ*, 436, 33
- Burles, S., Nollett, K. M., & Turner, M. S. 2001, *ApJ*, L1
- Cen, R. & Ostriker, J. P. 1999, *ApJ*, 514, 1
- Chen, H.-W., Lanzetta, K. M., Webb, J. K., & Barcons, X. 1998, *ApJ*, 498, 77
- _____. 2001, *ApJ*, 559, 1
- Chen, H.-W. & Prochaska, J. X. 2000, *ApJ*, 543, L9
- Chen, H.-W., Lanzetta, K. M., & Webb, J. K. 2001, *ApJ*, 556, 158
- Davé, R., Cen, R., Ostriker, J. P. et al. 2001, *ApJ*, 552, 473
- Ellingson, E. & Yee, H. K. C. 1994, *ApJS*, 92, 33
- Ellis, R. S., Colless, M., Broadhurst, T. et al. 1996, *MNRAS*, 280, 235
- Fabbiano, G., Kim, D.-W., & Trinchieri, G. 1992, *ApJS*, 80, 531
- Ferland, G. J. 1995, *HAZY*, a Brief Introduction to Cloudy (Univ. Kentucky Phys. Astron. Dept. Internal Rep.)
- Fukugita, M., Hogan, C. J., & Peebles, P. J. E. 1998, 503, 518
- Haardt, F., & Madau, P. 1996, *ApJ*, 461, 20
- Lanzetta, K. M., Bowen, D. V., Tytler, D., & Webb, J. K. 1995, *ApJ*, 442, 538
- Lanzetta, K. M., Webb, J. K., & Barcons, X. 1997, in *Proceedings of the 13th IAP Colloquium, Structure and Evolution of the Intergalactic Medium from QSO Absorption Line Systems*, eds. Petitjean and Charlot, p. 213
- Lilly, S. J., Tresse, L., Hammer, F. et al. 1995, *ApJ*, 455, 108
- Lopez, S., Reimers, D., Rauch, M., & Sargent, W. L. W. 1999, *ApJ*, 513, 598
- Mulchaey, J. S., Davis, D., Mushotzky, R., & Burstein, D. 1996, *ApJ*, 456, L5
- Pascarelle, S., Lanzetta, K. M., Chen, H.-W., & Webb, J. K. 2001, *ApJ*, 560, 1
- Prochaska, J. X. 1999, *ApJ*, 511, 71
- Prochaska, J. X. & Burles, S. M. 1999, *AJ*, 117, 1957
- Rauch, M., Miralda-Escud'e, J., Sargent, W. L. W. et al. 1997, *ApJ*, 489, 7
- Rauch, M. 1998, *ARA&A*, 36, 267
- Rauch, M., Sargent, W. L. W., & Barlow, T. A. 1999, *ApJ*, 515, 500
- Schramm, D. N. & Turner, M. S. 1998, *Review of Modern Physics*, 70, 303
- Shapiro, P. R. & Moore, R. T. 1976, *ApJ*, 207, 460
- Silk, J. & Norman, C. 1981, *ApJ*, 247, 59
- Spinrad, H., Filippenko, A. V., Yee, H. K. et al. 1993, *AJ*, 106, 1
- Spitzer, L. 1978, in *Physical Processes in the Interstellar Medium*
- Tripp, T. M., Savage, B. D., & Jenkins, E. B. 2000, *ApJ*, L1
- van Gorkom, J. 1993, in *The Evolution of Galaxies and Their Environment*, Proc. 3d Tetons Summer Astrophysics Conference, ed. J. M. Shull & H. A. Thronsons, Jr., p. 345
- Wang, X., Tegmark, M., & Zaldarriaga, M. 2001, *astro-ph/0105091*